

Nuclear Spin Saturation by Ultrasonics in Sodium Chloride†

E. F. TAYLOR* AND N. BLOEMBERGEN
Harvard University, Cambridge, Massachusetts

(Received September 8, 1958; revised manuscript received October 1, 1958)

An ultrasonic vibrational mode with rather well-defined properties has been set up in a cylindrical single crystal of sodium chloride. The saturation of the spin levels of Na^{23} and Cl^{35} by acoustically induced quadrupole transitions, $\Delta m = \pm 2$, has been measured in the steady state by a standard nuclear magnetic resonance technique, for several orientations of the ultrasonic wave and external magnetic fields. The components of the fourth-order tensor connecting the electrical field gradient tensor at the nuclei with the strain deformation tensor have been determined. The components satisfy an isotropy condition rather than the Cauchy relation. The results show the inadequacy of the ionic point-charge model coupled with an isotropic Sternheimer antishielding factor. The interpretation of the data requires a considerable amount of covalent character and configurational interaction on the Na^+ ion.

I. INTRODUCTION

THE interaction of acoustical waves with nuclear spins was first demonstrated by Proctor and co-workers.¹⁻³ A quantitative interpretation of their results has been hampered by insufficient knowledge about the configuration of the acoustical field. In a recent paper Jennings, Tanttila, and Kraus⁴ have pointed out that this difficulty does not exist if one is content with the ratio of the average over all orientations of the quadrupole interactions of two constituents in the same crystal. In their experiment on a sodium iodide crystal they were faced, however, with some uncertainty in the broadening of the I^{127} resonance by crystalline imperfections.

The object of the research reported in this paper is to measure with reasonable accuracy the components of the fourth-order tensor \mathbf{S} , connecting the electric field gradient tensor at the nucleus with the strain deformation tensor ϵ :

$$\nabla_i \nabla_j V = \sum_{k,l} S_{ijkl} \epsilon_{kl}(i, j, k, l = x, y, z). \quad (1)$$

This tensor \mathbf{S} is related in a straightforward manner by the elastic constants to the tensor \mathbf{C} introduced by Shulman *et al.*,⁵ which relates the electric field gradient to the stress tensor. The relationship with \mathbf{F} tensors introduced by Cohen and Reif⁶ will be discussed in the final section of this paper.

The nonvanishing components of \mathbf{S} , written in the

Voigt notation, satisfy the following conditions:

$$\begin{aligned} S_{11} = S_{22} = S_{33}, \quad S_{12} = S_{13} = S_{23} = S_{21} = S_{31} = S_{32}, \\ S_{44} = S_{55} = S_{66}, \quad S_{22} = -2S_{12}. \end{aligned} \quad (2)$$

The last relation follows from the requirement that the trace of the electric field gradient should vanish. The other relations follow from symmetry arguments.

In principle, the two independent components S_{11} and S_{44} can be determined by static deformation of the crystal and observation of the displacement and splitting of the resonance line. This method has been successful⁵ in InSb, but in the alkali halide crystals plastic flow and crystal failure occurs⁷ before appreciable effects are observed. The interest here is in a property of the perfect crystal.

Acoustical saturation can give the required information. A simple argument shows that the deformation required to get an observable saturation is $(T_2/T_1)^{1/2}$ times smaller than to get an observable static broadening of the resonance line. Furthermore it is simpler to get a uniform deformation, over regions small compared to the wavelengths, by ultrasonics than by static loading. The field gradient at the nucleus is mainly determined by the deformation in a region of a few interatomic distances, whereas the wavelength of an ultrasonic vibration at 10 Mc/sec is of the order of 10^{-2} cm. Therefore the acoustical deformations can be considered as uniform at each nucleus. An appropriate spatial average of the deformation tensor over the whole crystal must be taken to interpret the over-all saturation in the crystal.

The results are more informative than the measurement of the quadrupolar relaxation alone, because the spin-lattice relaxation time is determined by the combined deformations of all thermally excited phonons, rather than by a single acoustical mode of a wavelength long compared to the interatomic distances.

The quantities S_{11} and S_{44} can be determined from two (or more) different geometries of the acoustical field or the external magnetic field with respect to the crystallographic axes.

⁷ G. D. Watkins and R. V. Pound, Phys. Rev. **89**, 658 (1953).

† This work was performed in partial fulfillment of the requirements for the degree of Doctor of Philosophy of E. F. T. at Harvard University. It was supported jointly by the Office of Naval Research, Signal Corps, and the Air Force Office of Scientific Research.

* Present address: Wesleyan University, Middletown, Connecticut.

¹ W. G. Proctor and W. H. Tanttila, Phys. Rev. **98**, 1854 (1955).

² W. G. Proctor and W. H. Tanttila, Phys. Rev. **101**, 1757 (1956).

³ W. G. Proctor and W. Robinson, Phys. Rev. **104**, 1344 (1956).

⁴ Jennings, Tanttila, and Kraus, Phys. Rev. **109**, 1059 (1958).

⁵ Shulman, Wyluda, and Anderson, Phys. Rev. **107**, 953 (1957).

⁶ M. H. Cohen and F. Reif, in *Solid State Physics*, edited by F. Seitz and D. Turnbull (Academic Press, Inc., New York, 1957), Vol. 5, p. 350 ff.

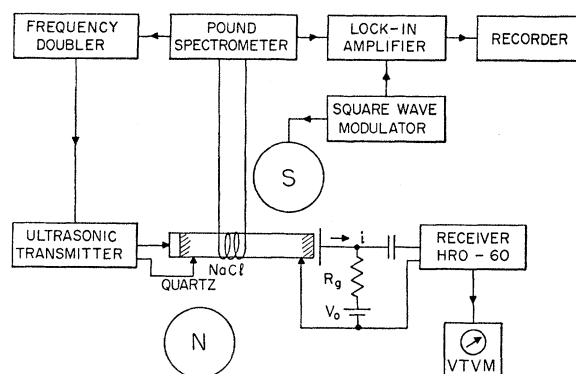


Fig. 1. Block diagram of experimental arrangement.

In the next section the experimental arrangement will be described. Particular attention will be given to the measurement of the acoustical strain distribution. The theory of ultrasonic saturation will be reviewed in Sec. III. A comparison with the experimental results will be made in Sec. IV. In the final section an attempt is made to interpret these results in terms of the electronic structure of NaCl. It will turn out that even for this crystal the simple ionic point-charge model is inadequate to explain the results.

II. EXPERIMENTAL

A block diagram of the experimental arrangement is shown in Fig. 1. The sample is placed between the pole pieces of a 6-in. Varian magnet. The inhomogeneity of the field over the sample volume is about one tenth of the line width.

The combination of a Pound-Knight-Watkins spectrometer, lock-in detector, and square-wave modulation of the magnetic field allows the recording of a pure absorption curve. The amplitude of the modulation is ten gauss, large compared to the line width, for 200 ma in the Helmholtz modulation coils delivered from 6AS7 tubes. The modulation frequency is 150 cps. To get a good square form, a positive current spike at the leading edge and a negative spike at the trailing edge is provided by thyatron tubes. The Na²³ resonance has been observed at 6.25 Mc/sec and 3.6 Mc/sec, the Cl³⁵ resonance only at the lower frequency. The saturation level of the center of the absorption curve is measured as a function of the intensity of the acoustical vibrations at twice the frequency of the Pound spectrometer. The acoustical intensity is monitored by the variation in capacitance of the end face of the vibrating crystal and a fixed, charged reference plate.⁸ The HRO-60 receiver is tuned to the acoustical frequency. Its local oscillator is frequency modulated, so that the level of input signal can be recorded with a vacuum tube volt-

⁸ P. S. Bordini, *Nuovo cimento* 4, 177 (1947). Bordini used an FM system instead of measuring directly the alternating voltage induced on the charged capacitor plate as is done in the present work.

meter. Some details of mounting and acoustical modes will now be discussed.⁹

A. Sample and Mounting

The sample, which was obtained from Harshaw Chemical Company, is a single crystal of sodium chloride cut in the form of a right circular cylinder one centimeter in diameter and five inches long. The [110] crystallographic direction lies along the axis of the cylinder. The ends were fine-ground to be plane and parallel by A. D. Jones Optical Company of Cambridge. Both ends and the sides of the sample along half an inch adjacent to each end are silvered using vacuum evaporation. An X-cut quartz crystal transducer, resonant at the frequency to be used and of the same diameter as the sample, is fixed to one end of the sample. The adhesive used is Dow Resin (276-V9 Blend 288), kindly supplied by H. J. McSkimin. This resin can be applied by raising the temperature of the sample to about 45°C. The bond is rather firm at room temperature, but quartz crystals can be interchanged by heating the sample again. Great care is taken that there are no dust particles on the end of the sample to which the quartz is joined.

The crystallographic orientation of the sample was determined by using x-rays. Since the [110] direction lies along the cylindrical axis of the sample, any of the directions [110], [001], or [111] can be made parallel to the steady magnetic field by simple rotation of the sample about its cylindrical axis.

When not in use, the sample is kept in a desiccator to prevent the absorption of moisture from the atmosphere.

The sample is placed between the pole pieces of a six-inch electromagnet in the mounting diagrammed in Fig. 2. At the left is the ultrasonic transmitter head. The lead from the quartz transducer is soldered to the center conductor of a type-N chassis connector to which the ultrasonic transmitter cable is connected. The sample rests on a knife edge which is in the form of a circle of larger diameter than the sample. The position of this knife edge can be adjusted vertically or laterally by loosening the screws which support it. A whisker of fine beryllium copper wire rests against the top of the sample to assure electrical contact with its silver plating. The transmitter head can be removed to allow for the introduction of the sample into the receiver head. During the experiment the transmitter head is clamped in place with a screw.

The nuclear resonance coil is wound on a fiber tube which is mounted in the first chamber in the receiver head. The sample fits through this tube without coming in contact with it. To prevent vibrational pickup by

⁹ E. F. Taylor, thesis, Harvard University, 1958 (unpublished). A more detailed description of the experimental equipment and procedure, and of the theoretical calculation of Sec. III, may be found in this thesis. Microfilm copies are available from the librarian of Lyman Laboratory.

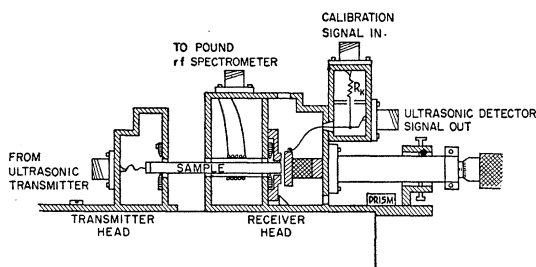


FIG. 2. Details of sample mounting (not to scale).

the coil, the entire chamber external to the fiber tube is filled with Hysol epoxy resin.

The remainder of the receiver head contains the variable capacitance ultrasonic detector and a calibration input. The plated lateral surface of the sample rests on a knife edge. A guard ring surrounds closely but does not touch the end of the sample. The face of the guard ring is optically fine-ground flat. During the experiment the end of the sample is flush with the end of this guard ring. Facing the end of the sample and the guard ring is a flat disk of beryllium copper which is also fine-ground optically flat. This is the high-voltage plate of the variable-capacitance ultrasonic detector. This plate is mounted on the end of an insulating polystyrene rod which is in turn mounted on a long beryllium copper rod which fits through a brass barrel. The separation between the end of the sample and the high-voltage capacitor plate is adjusted by means of a micrometer movement at the extreme right in Fig. 2. The parallelism of the end of the sample and the high-voltage plate can be adjusted to within a fraction of a thousandth of an inch by means of screws in the mounting of the brass barrel.

A total-reflecting prism is mounted near the micrometer movement at the right of the figure. This reflects light through a window at the bottom of the compartment. A front-silvered mirror reflects this beam up between the end of the sample and the high-voltage capacitor plate and out a second window in the top of the compartment. In this way the alignment of the end of the sample with the high-voltage plate and the coplanarity of the end of the sample with the face of the guard ring can be checked while the sample is mounted in the magnet.

A copper lead runs from the high voltage capacitance plate through a small chamber to a type-*N* chassis connector to which the receiver cable is attached. A resistor connects this high-voltage lead to a second type-*N* connector. This resistor and connector are used in the calibration of the ultrasonic signal.

All the chambers in the transmitter and receiver heads except for that containing the nuclear magnetic resonance coil have sides of one-sixteenth inch brass to prevent direct pickup of the ultrasonic transmitter signal by the receiver. The sides of the chamber con-

taining the nuclear magnetic resonance coil are covered by a 10-mil copper rf shield.

During the experiment small containers of silica gel desiccant are placed in the transmitter and receiver heads before attaching the side cover plates. In addition a plastic sheeting is scotch-taped in place to enclose the volume between the transmitter and receiver heads and another container of desiccant is placed in this enclosure. All of this precaution is to prevent the sodium chloride sample from absorbing moisture from the atmosphere.

B. Acoustical Modes

The basic theoretical work on axially symmetric vibrations in isotropic rods of infinite length was done in 1876 by Pochhammer.¹⁰ Solutions are of the form

$$w = \left[\frac{hA}{\beta^2 + h^2} J_1(hr) + \frac{j\beta C}{\beta^2 + k^2} J_1(kr) \right] \exp[j(\omega t - \beta x)],$$

$$u = \left[\frac{j\beta A}{\beta^2 + h^2} J_0(hr) + \frac{kC}{\beta^2 + k^2} J_0(kr) \right] \exp[j(\omega t - \beta x)],$$
(3)

where

$$\beta^2 = \frac{\omega^2}{v_x^2} = \frac{\rho\omega^2}{\lambda + 2\mu} - h^2 = \frac{\omega^2\rho}{\mu} - k^2,$$
(4)

and ρ is the density, v_x the velocity of propagation in the x direction, and λ and μ are the Lamé elastic constants.

In the above equations the propagation of the waves takes place in the x direction, u is the x displacement, and w is the radial displacement. Solutions for h and k and relative values for the amplitudes A and C are found by using Eq. (4), and by requiring that the radial and tangential stress on the surface of the cylinder be zero. The mathematical procedure for finding these roots has been treated by Hueter.¹¹ From Eq. (4) it can be seen that at any given frequency the velocity of propagation v_x will be slightly different for different solutions of h and k . The roots corresponding to modes of vibration most likely to be excited by the quartz transducer will be those for small h and real roots of k . If h should equal zero there would be no shear wave in the rod at all, only compressional waves. On the other hand, if k should equal zero, the only waves present would be shear waves.

The sodium chloride rod used in this experiment is neither isotropic nor infinite in length. Unfortunately the theory for a nonisotropic rod is prohibitively difficult. It would introduce an angular dependence around the direction of propagation, which will be ignored.

In a rod of finite length, with ends ground optically flat, one expects standing wave resonances if the

¹⁰ A. E. H. Love, *A Treatise on the Mathematical Theory of Elasticity* (Cambridge University Press, Cambridge, 1934).

¹¹ T. Hueter, *Z. angew. Phys.* 1, 274 (1949).

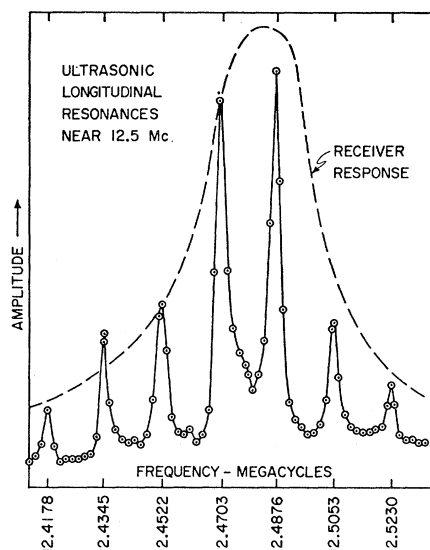


FIG. 3. Longitudinal resonances of NaCl bar near 12.5 Mc/sec. The bar contains about 700 half-wavelengths. The attenuation of a pulse during a single passage through this length is about 17%.

acoustical damping is small. Figure 3 shows the existence of these resonances. They are rather closely spaced, since the rod length corresponds to about 380 wavelengths. Evidence that these modes indeed correspond to the same set of h, k values of the Pochhammer equations is provided by measurement of the radial distribution of the displacement u . To this end, the condenser plate facing the end of crystal is divided into five insulated concentric rings of equal area. The relative displacement of the portion of the sample opposite each ring is related to the relative input voltage measured by the calibrated HRO receiver, when connected to each ring in turn. The step-wise radial distribution is the same for each acoustical resonance. A typical result is plotted in Fig. 4 (top), and it is seen that it corresponds closely to the radial distribution from the most uniform Pochhammer mode. The corresponding radial displacements w have not been measured but they should be much smaller, as the theoretical values of Fig. 4 (bottom) show.

At the higher frequency it is safe to assume that the variation of u over the volume of the rod is given by

$$u = A_0 Y(r) \cos \beta x e^{i\omega t}, \quad (5)$$

where $Y(r)$ is the normalized observed radial distribution function,

$$2r_0^{-2} \int_0^{r_0} Y(r) r dr = 1, \quad (6)$$

where r_0 is the radius of the sample. The dominant strain component is given by

$$\epsilon_{xx} = \partial u / \partial x = \beta A_0 \sin \beta x Y(r) e^{i\omega t}. \quad (7)$$

The other strain components amount to a few percent

of ϵ_{xx} according to theoretical estimates from Eqs. (3) and (4). The value of A_0 is related to the average displacement of the free end face, $\beta x = n\pi$, which is measured by the change in total capacitance,

$$A_0 = di / \omega C_0 V_0, \quad (8)$$

where i is the input current into the calibrated HRO-60 receiver. Its experimental range was $(0.7-11.0) \times 10^{-8}$ ampere. $V_0 = 185$ volts is the dc voltage applied to the condenser plate, $C_0 = 3.6 \mu\text{f}$ is the capacitance, $d = 0.02$ cm is the equilibrium distance between the condenser plate and the end face of the crystal. The average displacement of the free vibrating end of the crystal during acoustical saturation runs at 12.5 Mc/sec was between 2.5×10^{-9} cm and 4×10^{-8} cm. In this way an absolute value for the strain measurement is obtained, which permits an absolute determination of the components of the \mathbf{S} tensor, as discussed in the next section.

The modes at the lower acoustical frequency of 7.2 Mc/sec were less clean. Their spacing in frequency was not exactly equal and the radial distribution of the displacement in these modes was not identical. This variation in "cleanness" with frequency has been observed by other authors.¹² It is caused by interference effects between different Pochhammer modes. Although no accurate absolute values of the components of the strain tensor, nor therefore of the \mathbf{S} tensor, can be obtained at the lower frequency, it should be emphasized that the ratios S_{11}/S_{44} and $(S_{11})_{Na}/(S_{11})_{Cl}$ should still be obtained accurately. They are determined from saturation in an identical acoustical mode, by variation of the direction or magnitude of the external field.

III. THEORY OF ACOUSTICAL SATURATION

Consider the equally spaced energy levels of sodium and chlorine ($I = \frac{3}{2}$) in the external magnetic field H_0 .

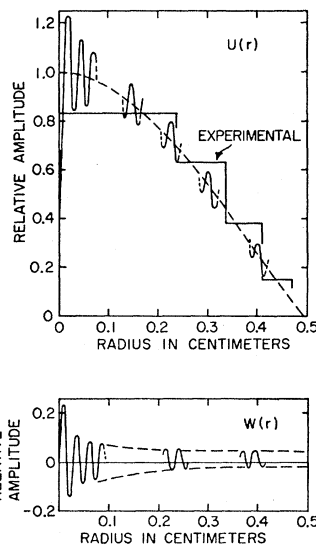


FIG. 4. Top: Theoretical distribution of the longitudinal displacement in the most uniform mode as a function of radius at 12.5 Mc/sec. Elastic isotropy is assumed. The step-averaged experimental distribution is shown for comparison. It is the same for all resonances shown in Fig. 3. Bottom: Theoretical distribution of the radial displacement in the same mode.

¹² H. J. McSkimin, J. Acoust. Soc. Am. 28, 484 (1956).

Consider the transitions induced by the ultrasonic wave, $\Delta m_I = \pm 2$, by the radiofrequency probing field of the spectrometer $\Delta m_I = \pm 1$, by the relaxation effects from paramagnetic impurities and from lattice vibrations, and flip-flops within the spin system $\Delta m_i = -\Delta m_j = \pm 1$ from spin-spin interactions. The processes are schematized in Fig. 5. The rate equations for the population in the four levels can be written down. The double spin-flip processes give rise to nonlinear terms, $P(n_1 n_3 - n_2^2)$, etc., but they can be linearized in the usual case that all population differences are small compared to the populations themselves. A steady state solution can be readily found because of the symmetry between the m_I and $-m_I$ levels and the trace relation $\sum n_m = N$. The observed absorption power is given by

$$g = W_{rf}(3n_1 + n_2 - n_3 - 3n_4)h\nu, \quad (9)$$

$$W_{rf} = \frac{1}{4}\gamma^2 H_{rf}^2 g(\nu), \quad (10)$$

$g(\nu)$ is the normalized line shape function. The complete solution for the populations will not be reproduced here because the results can be interpreted with a greatly simplified solution which has been discussed previously by Abragam and Proctor¹³ and by Kraus and Tanttilla.¹⁴ Note that the order of magnitude of P is T_2^{-1} , whereas $W_{1,2} \sim T_1^{-1}$ and $W_u, W_{rf} < 10T_1^{-1}$ even for 90% saturation. Since $T_2 \ll T_1$, the limit of the solution for $P \rightarrow \infty$ may be taken. The spin-spin interactions maintain at all times a Boltzmann distribution between the equidistant spin levels.¹⁵ The ratio of the imaginary part of the radiofrequency susceptibility in the presence of ultrasonic and radiofrequency saturation to the unsaturated value is

$$\frac{\chi''}{\chi_0} = \left[1 + \frac{W_u + (5/4)W_{rf}}{W_2 + \frac{1}{4}W_1 + (5/4)W_p} \right]^{-1}. \quad (11)$$

The saturation by the radiofrequency field was not negligible for optimum signal-to-noise ratio from the Pound spectrometer. The reduction in signal Z by this saturation alone was determined in a separate experiment without ultrasonics. The ratio of absorbed power in the presence and absence of ultrasonic saturation can then be written as

$$\frac{g}{g_0} = \left[1 + \frac{ZW_u}{W_2 + \frac{1}{4}W_1 + (5/4)W_p} \right]^{-1}. \quad (12)$$

The quantity W_u is proportional to the square of the ultrasonic strain. In the experimental arrangement a longitudinal standing wave in the x direction is used, corresponding to the $[110]$ direction in the crystal. The dc magnetic field H_0 along the z axis can be rotated in

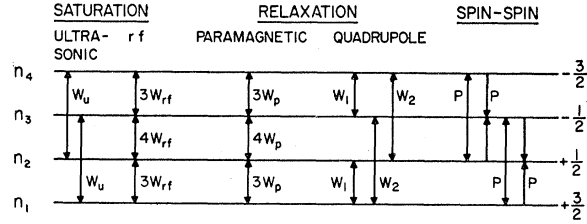


Fig. 5. Transitions between nuclear spin levels of Na^{23} or Cl^{35} . The various transition rates determine the populations n in each level. The diagram does not show that the probability of the relaxation processes is slightly different in opposite directions to insure a Boltzmann distribution in the absence of saturation.

a crystallographic (110) plane. The angle between H_0 and the $[110]$ direction is denoted by ϑ . The fourth order tensor which is given by Eqs. (1) and (2) if referred to the system of cubic crystallographic axes should be transformed to this new coordinate system. The resultant expression for the ultrasonic transition probability is

$$W_u = K \epsilon_{xx}^2 = \frac{3g(\nu)}{4\hbar^2} \left[\frac{eQ}{2I(2I-1)} \right]^2 \times \left[\frac{3}{4} \frac{S_{44}}{S_{11}} + \left(\frac{S_{44}}{S_{11}} - \frac{3}{4} \right) \sin^2 \vartheta \right] S_{11}^2 \epsilon_{xx}^2. \quad (13)$$

For a longitudinal wave along a cubic axis, perpendicular to H_0 , there would be no angular dependence of W_u , and the constant S_{44} could not be determined in that geometry. Since in the experiment the strain ϵ_{xx} has a spatial variation, an average of the absorbed power over the sample should be taken. The saturation will have a spatial variation. It is known that spin-spin diffusion will tend to smooth out this variation. However, the time for spin diffusion to be effective over an acoustic wavelength λ is $T_2(\lambda^2/a^2) \gg T_1$ so that it can be neglected. The square of the strain will be taken as

$$\epsilon_{xx}^2 = \beta^2 A_0^2 \sin^2 \beta x [Y(r) + 0.05]^2. \quad (14)$$

The constant 0.05 is added to represent the effect of other strain components.

Furthermore, the effect of the square-wave on-off modulation should be considered. Strictly speaking, one should not take the steady-state solution, but the combination of exponential decay and growth curves. Since the modulation frequency is fast compared to W_u, W_{rf} , and T_1^{-1} one may say that the on-off modulation reduces the effective values of W_u and W_{rf} by a factor $\frac{1}{2}$.

Theoretical expressions for W_1 and W_2 have been given by van Kranendonk¹⁶ and others.¹⁷⁻¹⁹ They are

¹⁶ J. van Kranendonk, *Physica* **20**, 781 (1954).

¹⁷ Das, Roy, and Ghosh, *Phys. Rev.* **104**, 1568 (1956).

¹⁸ E. G. Wikner and T. P. Das, *Phys. Rev.* **109**, 360 (1958).

¹⁹ K. Yosida and T. Moriya, *J. Phys. Soc. (Japan)* **11**, 33 (1956). The authors consider a different experimental situation in this paper. Only $m = \frac{1}{2} \rightarrow -\frac{1}{2}$ transitions are induced by the applied field. Their saturation formula is therefore different from Eq. (11).

¹³ A. Abragam and W. G. Proctor, *Phys. Rev.* **109**, 1441 (1958).

¹⁴ O. Kraus and W. H. Tanttilla, *Phys. Rev.* **109**, 1052 (1958).

¹⁵ N. Bloembergen, *Proceedings of the International Conference on Theoretical Physics*, Kyoto, 1953 (Science Council of Japan, Tokyo, 1954), p. 757.

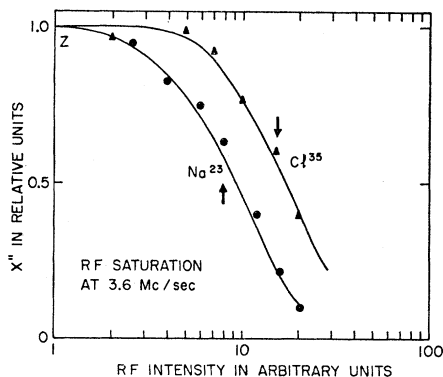


FIG. 6. Saturation curves for Na^{23} and Cl^{35} in the absence of ultrasonic power. The arrows indicate the radiofrequency power, at which the ultrasonic saturation curves in Fig. 7 were taken.

not helpful for the problem at hand, the determination of the \mathbf{S} -tensor, because they contain similar undetermined constants relating the deformations in lattice vibrations to the electric field gradients. Experimental relaxation times should be used to eliminate the quantities W_1 , W_2 , and W_p . In principle they can be separated by measurement of the relaxation time at different temperatures and frequencies. At room temperature a simple exponential recovery of the magnetization is observed defining a single spin-lattice relaxation time T_1 . This is to be expected for the four equally spaced levels. It can be shown from the rate equations for the populations that

$$(8/5)T_1 = [\frac{1}{4}W_1 + W_2 + (5/4)W_p]^{-1}. \quad (15)$$

Substitute Eqs. (14) and (15) into (13) and (12) and take an average of (12) over the volume of the sample. The average over the acoustical wavelength, i.e., the integration over x , can be carried out explicitly and the result is

$$\langle g/g_0 \rangle = 2r_0^{-2} \int_0^{r_0} \{1 + \frac{4}{5}\beta^2 A_0^2 [Y(r) + 0.05]^2 K Z T_1\}^{-\frac{1}{2}} r dr. \quad (16)$$

This integral is evaluated numerically with the experimental step function for $Y(r)$.

IV. EXPERIMENTAL RESULTS

Saturation curves at 3.6 Mc/sec of the rf spectrometer, in absence of ultrasonic waves, are shown in Fig. 6. From it the factor Z is determined for the Na^{23} and Cl^{35} resonance. A similar curve was obtained for the Na^{23} resonance at 6.25 Mc/sec. The spin-lattice relaxation time T_1 for Na^{23} was measured directly with pulse equipment described by Sorokin.²⁰ The resulting value is $T_1 = 12.4 \pm 1.0$ sec.

The line width $\Delta\nu$ between points of maximum and minimum slope has also been measured. It is related to the maximum of the shape function, if the latter is

²⁰ N. Bloembergen and P. P. Sorokin, Phys. Rev. **110**, 865 (1958).

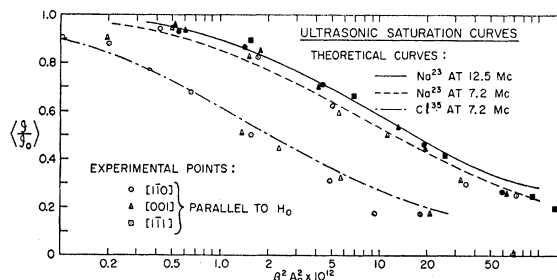


FIG. 7. The relative value of the nuclear susceptibility as a function of the ultrasonic intensity at twice the radiofrequency. The solid experimental points are for Na^{23} ultrasonic saturation at 12.5 Mc/sec. The drawn curve is calculated with Eq. (16). The open experimental points are for Na^{23} and Cl^{35} ultrasonic saturation at 7.2 Mc/sec. The dotted curves are calculated with Eq. (16).

assumed to be Gaussian, by

$$g_{\max}(\nu) = (2/\pi)^{\frac{1}{2}} \Delta\nu^{-1}.$$

Values of $\Delta\nu$ can be found in the fourth column of Table I.

The ultrasonic saturation data are shown in Fig. 7. The dotted curves correspond to the theoretical expression (16) with the best values of K for the Na^{23} and Cl^{35} resonance at an ultrasonic frequency of 7.2 Mc/sec. It is seen that there is no angular dependence in these saturation curves. The experimental points are similar for H_0 parallel to $[001]$, $[0\bar{1}1]$, and $[\bar{1}\bar{1}1]$. According to Eq. (13) this implies $S_{44}/S_{11} = \frac{3}{4}$. This may be called the isotropy condition for the \mathbf{S} -tensor. It can be compared with the corresponding relation between the elastic moduli to insure the same acoustical velocity in all directions. The values of the quadrupole moments^{21,22} are listed in the second column.

The absolute values of S_{11} are derived from the best value of K with Eq. (13) and appear in column 8. A serious source of error in the design of our calibration circuit to determine the value of the input current i in Eq. (8) was pointed out to us²³ after the experimental work was substantially completed. A recalibration to take account of stray capacitance has been carried out afterwards. The results quoted here differ appreciably from those reported earlier.⁹ The calibration error may still be as large as a factor two. Inherently the method is capable of a much higher accuracy and further work to determine the absolute values of S_{11} is planned. It should be emphasized that the ratios S_{44}/S_{11} and $(S_{11})_{\text{Na}}/(S_{11})_{\text{Cl}}$ are not affected by this uncertainty.

The corresponding data for the Na^{23} ultrasonic saturation at 12.5 Mc/sec are also given. The best-fit theoretical saturation curve is drawn. The value of S_{11} is somewhat lower, although it is the same within the limits of error, than at 7.2 Mc/sec. The discrepancy in the tail between the experimental and theoretical

²¹ V. Jaccarino and J. G. King, Phys. Rev. **83**, 471 (1951).

²² Perl, Rabi, and Senitzky, Phys. Rev. **98**, 611 (1955).

²³ We wish to thank Dr. Menes and Dr. Proctor for pointing out this source of error.

TABLE I. Ultrasonic saturation data.

Nucleus ultrasonic frequency	Q cm ²	T_1 sec	$\Delta\nu$ cycles/sec	Z	S_{44}/S_{11}	$S_{11}(\text{Cl})/S_{11}(\text{Na})$	S_{11} statcoul/cm ³	$1+\gamma_\infty$ exper.	$1+\gamma_\infty$ calculated ^{a,b}
³⁵ Cl									
7.2 Mc/sec	0.8×10^{-25} ^c	10.0 ± 2	870 ± 50	0.60 ± 0.05	0.75 ± 0.1	$1.8 \pm 20\%$	2.3×10^{15}	9	50 to 57
²³ Na									
7.2 Mc/sec	1×10^{-25} ^d	12.4 ± 1	2800 ± 200	0.64 ± 0.05	0.75 ± 0.1		1.3×10^{15}	5	5.5
²³ Na									
12.5 Mc/sec	1×10^{-25}	12.4 ± 1	2800 ± 200	0.50 ± 0.1	0.75 ± 0.1		1.1×10^{15}	4	5.5

^a See reference 18.

^b See reference 24.

^c See reference 21.

^d See reference 22.

saturation curves should be ascribed to the effect of impure acoustical modes. In the tail most of the signal comes from the regions in the standing-wave pattern where the acoustical strain is small. Here saturation from the presence of unwanted modes will cause the experimental points to fall below the theoretical curve.

A comparison of the radiofrequency and ultrasonic saturation curves for Na²³ and Cl³⁵ is interesting. The former give for the ratio of the relaxation times, $T_1(\text{Cl})/T_1(\text{Na})=0.8$. Wikner²⁴ finds 0.45 from echo decay curves. If the assumption is made that relaxation by paramagnetic impurities is negligible, $W_p=0$, and if the deformations from the high-frequency lattice vibrations and low-frequency ultrasonic waves are related to the resulting electric field by the same S -tensor, one would have

$$\frac{T_1(\text{Cl})}{T_1(\text{Na})} = \frac{S_{11}^2 Q^2(\text{Na})}{S_{11}^2 Q^2(\text{Cl})}$$

This gives a ratio of 0.65. The reasonable agreement between the three independent experimental methods supports the validity of the assumptions stated above. It is not correct to conclude that the ultrasonic amplitude A_0 to produce a given amount of saturation should be the same for Na and Cl. The distinction is that the lattice vibrations provide a continuous spectral density whereas the ultrasonic vibration is a pure harmonic. What should be the same for both nuclear species is the product $A_0^2(50\% \text{ sat})Z(\Delta\nu)^{-1}$, and this is approximately fulfilled. It is not clear whether the small discrepancy should be ascribed to a small contribution from paramagnetic impurities and spin diffusion to the Na relaxation, or to a different relationship between the deformation and gradient tensors when the wavelength of the lattice vibrations is comparable to the interatomic distance.

V. DISCUSSION IN TERMS OF ELECTRONIC THEORY

It remains to explain the observed values of S_{11} and S_{44} in terms of the electronic structure of NaCl. The

²⁴ The experimental value for T_1 for Na²³ in NaCl in the table of reference 18 should read 12 sec instead of 7 minutes; the value T_1 for Cl³⁵ in NaCl is 5.3 sec; E. G. Wikner (private communication).

model which has been used most extensively is that of a free ion surrounded by a lattice of point charges. The gradient produced by the charges in the deformed lattice has been discussed by Cohen and Reif.⁶ It can be calculated from the potential in the deformed lattice of point charges by differentiation, and should be multiplied by the Sternheimer (anti)shielding factor²⁵ $(1+\gamma_\infty)$ to obtain the gradient at the nucleus inside the ion. For the NaCl structure it is found that

$$S_{11} = 11.8(1+\gamma_\infty)ea^{-3}, \quad (17)$$

where e is the charge on the neighboring ion and a is the interionic distance. It is interesting to note that the contribution of the six neighboring ions alone is almost the same as the total sum. In the six-point-charge model, 11.8 is replaced by 12.

The ratio $S_{44}/S_{11} = -\frac{1}{2}$ for the cubic point-charge lattice. This may be called the Cauchy relation for the S -tensor. Apparently there is violent disagreement between this relation and the observed isotropy relation $S_{44}/S_{11} = +\frac{3}{4}$. It is also seen that the experimental ratio $(S_{11})_{\text{Cl}}/(S_{11})_{\text{Na}} = 1.8$ whereas the relation (17) would predict a factor 10. The inadequacy of the pure ionic model is not surprising, as data for the chemical shift and electron-coupled nuclear-spin interactions^{19,20} have also indicated the presence of appreciable deviations from the pure ionic states. The distortions may be described in terms of overlap integrals or of admixture of covalent orbitals.

The absolute value of S_{11} for Na⁺ comes close to the value calculated by Eq. (17) with the Sternheimer γ_∞ . Kawamura²⁶ derived a value of S_{11} from static quadrupole broadening of the Na²³ resonance in a mixed crystal NaCl-NaBr. His experimental value is in agreement with ours. However, if the theory of van Kranendonk¹⁶ for the spin-lattice relaxation time is used with the ionic model, Wikner and Das¹⁸ find that $T_1 = 25$ minutes, whereas the observed value is 12.4 sec.²⁴

The observed quadrupole coupling for Cl³⁵ is considerably smaller than predicted by Eq. (17). This is the usual situation for halogen couplings in alkali

²⁵ R. M. Sternheimer and W. H. Foley, Phys. Rev. **102**, 731 (1956).

²⁶ Kawamura, Otsuka, and Ishitawara, J. Phys. Soc. Japan **11**, 1064 (1956).

molecules.¹⁸ On the other hand, the Na²³ coupling in the NaCl molecule is at least an order of magnitude larger²⁷ than the ionic model would predict. There is no direct correlation between the molecules and the corresponding crystal lattice. In either case, the ionic model is inadequate to explain all observed couplings. It also fails to account for the large chemical shifts of the metal ions in alkali halide crystals. It should be emphasized that the model even fails to give the correct ratio of coupling constants. The fair agreement obtained by Jennings⁴ in NaI is probably fortuitous.

It appears that only elaborate calculations, such as those of Löwdin²⁸ for the elastic constants, can be

²⁷ Honig, Mandel, Stitch, and Townes, *Phys. Rev.* **96**, 629 (1954).

²⁸ P.-O. Löwdin, thesis, Uppsala, 1948 (unpublished). *Note added in proof.*—Kondo and Yamashita [*J. Phys. Chem. Solids* (to be published)] have very recently carried out such a program. It appears that in general a combination of the overlap effect and the effects considered in references 18 and 19 is necessary to obtain agreement with experimental results.

expected to give reliable results for the *S*-tensor. The relationship of this tensor with the photoelastic effect²⁹ has been pointed out by Cohen and Reif.⁶ The model of the deformed lattice of point charges has to be supplemented, however, by the assumption of anisotropy of the ionic polarizability in the deformed lattice. This phenomenological description again points up the inadequacy of the pure ionic model. Valence orbitals which contribute much to the polarizability and to electric field gradient at the nucleus are very sensitive to deformation. That is the reason for the failure of the Cauchy relation for the *S*-tensor and the photoelastic tensor. On the other hand, the valence orbitals contribute little to the binding energy, which consists mainly of electrostatic energy and ion core deformation. The elastic constants in NaCl therefore obey the Cauchy relation very well.³⁰

²⁹ H. Mueller, *Phys. Rev.* **47**, 947 (1935).

³⁰ C. Kittel, *Introduction to Solid State Physics* (John Wiley and Sons, Inc., New York, 1956), second edition, Chap. 4.

Effect of Pressure on Anelastic Relaxation in Silver-Zinc*

G. W. TICHELAAAR AND D. LAZARUS

Department of Physics, University of Illinois, Urbana, Illinois

(Received September 22, 1958)

Using a novel experimental apparatus, studies have been made of the effect of hydrostatic pressure up to 9000 kg/cm² on the rate of stress relaxation at constant small strain in an Ag-30 atomic percent Zn alloy, where the relaxation process is presumably diffusion limited. For temperatures between 110°C and 150°C the relaxation time is found to increase exponentially with pressure. The zero-pressure data are in good agreement with previous work by Nowick. At 9000 kg/cm² the relaxation time is about a factor of four greater than at 1 kg/cm², for all temperatures. The pressure dependence can be interpreted in terms of an "activation volume" of 5.36 ± 0.07 cm³/mole, which is about half the atomic volume of the material. This may mean that the volume of formation of a vacancy is at most about half of the molar volume, which number is in accordance with a recent calculation by Tewordt.

INTRODUCTION

IN recent years considerable evidence has been accumulated to substantiate the vacancy mechanism for volume diffusion in metals.¹ Most of the experimental work has involved radioactive tracer measurements of the diffusion coefficients of the atoms, while determination of the change in resistivity² and anelastic effects³ in quenched specimens has given more direct information about the vacancies. Various calculations have been made of the energy required to create and move a vacancy, which are in fair agreement with the experimental results. One major difficulty encountered in theoretical treatments is the consideration of relaxation

of the lattice about a vacancy. It has often been assumed that in a face-centered cubic lattice the amount of relaxation would be very small.⁴ Recently, Tewordt,⁵ in a detailed calculation of the elastic strains about point defects, has shown that, in copper, the volume of the vacancy may be as small as 50% of the atomic volume.

No direct measurements have been made of the volume of defects. Bauerle and Koehler² measured simultaneously the change in length and resistivity in quenched gold wires, but were unable to establish the vacancy volume uniquely because of the uncertainty in the theoretical value of the specific resistivity of the defect.

Measurements of diffusion at high pressure offer a possible method for a fairly direct determination of

* Supported in part by the U. S. Atomic Energy Commission.

¹ F. Seitz, in *Phase Transformations in Solids* (John Wiley and Sons, Inc., New York, 1951), edited by R. Smoluchowski *et al.* pp. 77-148.

² J. E. Bauerle and J. S. Koehler, *Phys. Rev.* **107**, 1493 (1957).

³ A. S. Nowick and R. J. Sladek, *Acta Met.* **1**, 131 (1953).

⁴ H. B. Huntington, *Phys. Rev.* **61**, 325 (1942); A. Seeger and H. Bross, *Z. Physik* **145**, 161 (1956).

⁵ L. Tewordt, *Phys. Rev.* **109**, 61 (1958).